

## Vortex-Line-Lattice Melting, Vortex-Line Cutting, and Entanglement in Model High- $T_c$ Superconductors

Ying-Hong Li and S. Teitel

*Department of Physics and Astronomy, University of Rochester, Rochester, New York 14627*

(Received 15 January 1991)

We have carried out a Monte Carlo study of anisotropic 3D uniformly frustrated  $XY$  models, as a model for the type-II high- $T_c$  superconductors. Vortex-line-lattice melting, vortex-line cutting, and entanglement have been studied in relation to the superconducting phase transition.

PACS numbers: 74.60.Ge, 64.60.-i, 74.40.+k

One of the main foci of recent research on the type-II high- $T_c$  superconductors has concerned the fluctuation of vortex lines in the mixed phase. Because of the relatively large values of  $T_c$  and  $\kappa$ , it is believed that the vortex-line lattice will melt at a temperature well below that given by the mean-field  $H_{c2}(T)$  line.<sup>1</sup> Nelson<sup>1(a),2</sup> has proposed a theory of vortex-line fluctuations in the line liquid phase, based on an analogy with interacting bosons. Interesting dynamical effects have been suggested, based on an estimate yielding a high energy barrier for vortex-line cutting.<sup>1(a),2,3</sup> In such a case, a single pinned line would effectively pin those with which it is entangled, resulting in decreased flux-flow resistance in the liquid phase. Brandt<sup>1(c),4</sup> has questioned several features of this model, in particular, the estimated high barrier for line cutting. Feigel'man<sup>5</sup> has suggested an intermediate disentangled liquid phase, arising from the long-range interaction between lines near  $H_{c2}$ .

In view of these works, it is useful to have a well-defined microscopic model in terms of which vortex-line-lattice melting, vortex-line cutting, and the properties of the vortex-line liquid may be quantitatively examined. In this Letter we present such an investigation based on simulations of the three-dimensional uniformly frustrated anisotropic  $XY$  model on a cubic lattice. We consider the case where there are no random pinning impurities. We find clear evidence that at the superconducting transition, the vortex-line lattice melts into an entangled liquid. Transverse fluctuations of the vortex lines in the liquid phase are found to scale like a free random walk and the "entanglement correlation length"  $\xi_z$  is computed. Substantial vortex-line cutting is found in the liquid phase.

The Hamiltonian of our model is given by

$$\mathcal{H} = - \sum_{\langle ij \rangle} J_{ij} \cos(\theta_i - \theta_j - A_{ij}), \quad (1)$$

where  $\theta_i$  is the phase of the superconducting wave function at site  $i$ ,  $A_{ij} \equiv (2e/\hbar c) \int_j^i \mathbf{A} \cdot d\mathbf{l}$  is the integral of the vector potential from site  $i$  to site  $j$ , and the sum is over nearest-neighbor sites. We use a uniform magnetic induction  $\mathbf{B} = \nabla \times \mathbf{A}$  along the  $z$  direction, for which the sum of  $A_{ij}$  around a face of any cubic unit cell obeys the

constraint

$$A_{ij} + A_{jk} + A_{kl} + A_{li} = \begin{cases} 2\pi f, & \text{face in } x-y \text{ plane,} \\ 0, & \text{otherwise,} \end{cases} \quad (2)$$

where  $f = Ba^2/\Phi_0$  is equal to the average density of field-induced vortex lines ( $a$  is the lattice constant,  $\Phi_0$  is the flux quantum). Anisotropy may be introduced in the model by taking

$$J_{ij} = \begin{cases} J_{\perp} & \text{in } x-y \text{ plane,} \\ J_{\parallel} & \text{along } z \text{ direction.} \end{cases} \quad (3)$$

This model describes a lattice version of a type-II superconductor. The "bare" coherence length is  $\xi_0 \approx a$ , and the bare magnetic penetration length  $\lambda$  is given by  $J_{\perp, \parallel} = \Phi_0^2 a / 16\pi^3 \lambda_{\perp, \parallel}^2$ , where by bare we mean the values before renormalization due to fluctuations. Our approximation of replacing the spatially varying magnetic induction by its average value  $\mathbf{B}$  is reasonable in the limit  $a_v \ll \lambda$ , where  $a_v \sim \sqrt{f}$  is the average separation between vortex lines. We may see this explicitly by considering the interaction between two vortex lines in our model (1); for the isotropic case, a standard duality transformation<sup>6</sup> gives  $2\pi J \int d\mathbf{r}_1 \cdot d\mathbf{r}_2 V(\mathbf{r}_1 - \mathbf{r}_2)$ , where  $V(\mathbf{r})$  is the lattice Green's function which has Fourier transform<sup>7</sup>  $V_q = 1/q^2$ . In contrast, the London model gives an interaction<sup>4</sup>  $V_q = 1/(q^2 + \lambda^{-2})$ . Thus, while our model reduces vortex-line density fluctuations on long length scales  $r \gg \lambda$  ( $q \ll \lambda^{-1}$ ), fluctuations on scales  $r \ll \lambda$  are well approximated. When  $a_v \ll \lambda$ , our model should be reasonable for describing the small-length-scale fluctuations responsible for melting, and the collisions between neighboring vortex lines. As the high- $T_c$  materials are strongly type-II with  $\kappa \equiv \lambda/\xi_0 \gg 1$ , this condition should be satisfied for a wide range of magnetic field below  $H_{c2}$ , provided one is still well above  $H_{c1}$ .<sup>5</sup>

The vortex lines have well-defined identities in our model. By summing the gauge-invariant phase around the faces of cubic unit cells,  $\sum_{\text{face}} (\theta_i - \theta_j - A_{ij}) = 2\pi(n_a - f_a)$ , the integer vorticity  $n_a$  of each face  $a$  is determined. Here we restrict  $\theta_i - \theta_j - A_{ij} \in (-\pi, \pi)$  and  $f_a$  is the flux through the face ( $f_a = f$  in  $x-y$  plane,  $f_a = 0$  otherwise). The trace of a vortex line is then determined

by following this vorticity going in and coming out of the cubic unit cells of the lattice. The form of the interaction between bent vortex lines in this model is not presumed, but completely determined by the energetics of the microscopic variables  $\{\theta_i\}$ .

We consider here the special case of  $f = \frac{1}{5}$ . In the ground state, the vortex lines form a periodic square lattice<sup>8</sup> with  $a_v = \sqrt{5}a$  (see inset of Fig. 1). The triangular Abrikosov lattice found in the continuum is distorted here due to commensurability effects with the underlying cubic lattice of the model. To investigate the behavior of the model, we have used Monte Carlo (MC) simulations with the standard Metropolis algorithm applied to the Hamiltonian (1). Simulations have been carried out on  $L \times L \times (L_z + 1)$  cubic lattices with periodic boundary conditions in the  $x$ - $y$  plane and free boundary conditions in the  $z$  direction. We have used  $L = 10$  and  $L_z = 10, 15$ , and  $20$ . A wide range of anisotropy  $\gamma \equiv J_{\parallel}/J_{\perp} = 0.01 - 1.0$  was studied. Typically, 20000–30000 MC sweeps were used for averaging, after an initial 5000 for equilibration. Henceforth, energy scales will be quoted in units of  $J_{\perp}$ , and lengths in units of  $a$ .

We first focus our discussion on the isotropic case. The superconducting to normal transition can be characterized by the vanishing of the helicity modulus  $Y$  (analogous to the superfluid density; also  $Y \sim 1/\lambda_R^2$ , where  $\lambda_R$  is the renormalized magnetic penetration length).  $Y$  in direction  $\hat{\mu}$  in the  $x$ - $y$  plane is given by<sup>9</sup>

$$Y_{\hat{\mu}} = \frac{1}{N} \left\langle \left[ \sum_{\langle ij \rangle} J_{ij} \cos(\theta_j - \theta_i - A_{ij}) (\hat{\mathbf{e}}_{ij} \cdot \hat{\mu}) \right]^2 \right\rangle - \frac{1}{TN} \left\langle \left[ \sum_{\langle ij \rangle} J_{ij} \sin(\theta_j - \theta_i - A_{ij}) \hat{\mathbf{e}}_{ij} \cdot \hat{\mu} \right]^2 \right\rangle, \quad (4)$$

where  $\hat{\mathbf{e}}_{ij}$  is the unit vector from  $i$  to  $j$ , and  $N = L^2(L_z + 1)$ . The specific heat  $C$  is calculated using the usual fluctuation dissipation relation. Our results for  $Y$  (averaged over  $\hat{\mu} = \hat{x}, \hat{y}$ ) and  $C$  as functions of temperature  $T$

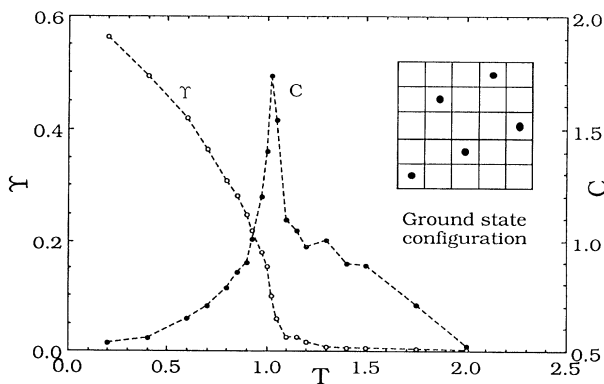


FIG. 1. Helicity modulus  $Y$  and specific heat  $C$  vs temperature  $T$ .  $Y \rightarrow 0$  defines the superconducting transition at  $T_c \approx 1.0$ . Inset: A top view of the ground-state vortex-line lattice. Dots give the positions of the parallel vortex lines.

for a  $10 \times 10 \times 21$  lattice are shown in Fig. 1. We find  $Y$  vanishes where  $C$  has its peak, giving  $T_c \approx 1.0$ , well below the mean-field value<sup>10</sup>  $T_c^{\text{MF}} \approx 2.5$ . Fluctuations are clearly strong and important in this model.

Next we consider the melting of the vortex-line lattice. The average transverse fluctuation of the vortex lines  $\langle u^2 \rangle$  is given by

$$\langle u^2 \rangle = \frac{1}{N_l L_z} \sum_{i=1}^{L_z} \langle [\mathbf{r}_i(z) - \mathbf{r}_i(z_0)]^2 \rangle, \quad z_0 = L_z/2, \quad (5)$$

where  $\mathbf{r}_i(z)$  is the position of vortex line  $i$  in the  $x$ - $y$  plane at  $z$ , and  $N_l = fL^2$  is the number of lines. Below the melting temperature, the vortex lines can only vibrate about their equilibrium positions. In the limit of  $L_z \rightarrow \infty$ ,  $\langle u^2 \rangle$  should approach a finite-temperature-dependent constant. Above the melting temperature, in an entangled liquid phase, the transverse fluctuation of a vortex line is expected to behave like a random walk in the interaction field of all other vortex lines.  $\langle u^2 \rangle$  should scale with  $L_z$  as a power law,  $\langle u^2 \rangle \sim L_z^{\nu_L}$ . The crossover between these two types of behaviors gives the melting temperature.

In Fig. 2, we plot  $\langle u^2 \rangle$  vs  $T$  for  $L_z = 5, 10, 15$ , and  $20$ .<sup>11</sup> By the above criterion, vortex-line-lattice melting to an entangled liquid is clearly seen to occur at  $T_c \approx 1.0$ , the same temperature at which  $Y \rightarrow 0$ . Thus vortex-line-lattice melting coincides with the loss of long-range phase coherence. A comparison of cooling versus heating showed no hysteresis. At  $T_c$  we find  $\langle u^2 \rangle^{1/2}/a_v \approx 0.45$ . Fitting our data above  $T_c$  with the form  $\langle u^2(T, L_z) \rangle = D(T)L_z^{\nu_L} + u_0^2(T)$ , we find scaling consistent with the prediction<sup>1(a)</sup>  $\nu_L = 1$  (see inset to Fig. 2). Thus, although the bare interaction between vortex lines is long range, for  $T > T_c$  the fluctuations of the vortex lines screen the interaction so that the transverse motion

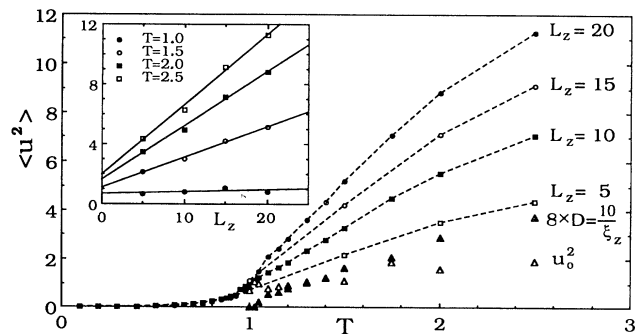


FIG. 2. Average transverse fluctuation  $\langle u^2 \rangle$  vs  $T$  for  $L_z = 5, 10, 15$ , and  $20$ . For  $T < T_c \approx 1.0$ ,  $\langle u^2 \rangle$  is independent of  $L_z$ , indicating a vortex-line lattice. For  $T > T_c$ ,  $\langle u^2 \rangle$  increases with  $L_z$ , indicating a vortex-line liquid. Inset:  $\langle u^2 \rangle$  vs  $L_z$ , for several  $T > T_c$ , demonstrating the free random-walk scaling behavior  $\langle u^2 \rangle = D(T)L_z^{\nu_L} + u_0^2(T)$  (solid lines are best fits). Fitted parameters  $D$  and  $u_0^2$  are also shown.  $D$  is related to the "entanglement" length  $\xi_z$  by  $D \approx 5/4\xi_z$ .

of a given line behaves like a simple free random walk. Our fitted parameters  $D(T)$  and  $u_0^2(T)$  are shown in Fig. 2. The diffusion constant  $D$  defines the "entanglement" length,<sup>1(a)</sup>  $\xi_z \approx (\frac{1}{2} a_c)^2/D(T)$ , which is the average length it takes to fluctuate half the distance  $a_c$ , the average spacing between vortex lines.

To further characterize the properties of the vortex-line liquid phase, we compute the line cutting density  $n_c$ , and the mutual winding number of pairs of lines  $w$ .  $n_c$  is straightforwardly defined as

$$n_c = \langle N_c \rangle / N_l, \quad (6)$$

where  $N_c$  is the number of cubic unit cells through which two or more vortex lines pass. When two vortex lines intersect in one cell, the choice of connections between incoming and outgoing lines for the purpose of determining the  $\mathbf{r}_i(z)$  of Eqs. (5) and (7) is made randomly.  $w$  is defined as

$$w = \frac{1}{N_l} \sum_{i \neq j} \left\langle \left| \sum_z \Theta(\mathbf{r}_i(z), \mathbf{r}_j(z)) \right| \right\rangle, \quad (7)$$

where the sum is over all pairs of vortex lines, and  $\Theta(\mathbf{r}_i(z), \mathbf{r}_j(z)) \in (-\pi, \pi]$  is the angle between the vectors  $\Delta \mathbf{r}(z) \equiv \mathbf{r}_i(z) - \mathbf{r}_j(z)$  and  $\Delta \mathbf{r}(z-1)$ .  $w$  increases by  $\pm \pi$  each time a given line crosses close to another line.<sup>12</sup> Hence  $w \approx \pi$  if on average each vortex line twists with one other line by a full turn, in going down the length  $L_z$  of the system.

Our results for  $n_c/L_z$  and  $w$  are plotted in Fig. 3. For  $T < T_c$ ,  $n_c \approx 0$ , and  $w < \pi$  is independent of  $L_z$  indicating no significant entanglement. For  $T > T_c$ ,  $n_c/L_z$  increases rapidly and is independent of  $L_z$ , giving a constant density of cuttings per unit length in the  $L_z \rightarrow \infty$  limit. Comparing Figs. 2 and 3(a), we find that the cutting length  $L_z/n_c$  is comparable to the entanglement length  $\xi_z$ , ex-

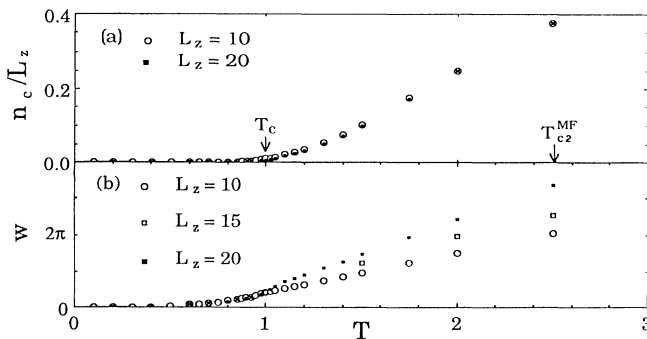


FIG. 3. (a) Cutting number per unit length  $n_c/L_z$  vs  $T$ .  $n_c \approx 0$  for  $T < T_c$  and grows rapidly for  $T > T_c$ , scaling linearly with  $L_z$ . (b) Mutual pair winding number  $w$  vs  $T$ . For  $T < T_c$ ,  $w < \pi$  is independent of  $L_z$ , indicating no entanglement. For  $T > T_c$ ,  $w$  increases with  $L_z$ . Comparing (a) and (b), one sees substantial vortex-line cutting once the lines are entangled ( $w \gtrsim \pi$ ). The transition temperature  $T_c$  and the mean field  $T_c^{\text{MF}}$  are indicated for comparison.

cept possibly for a very narrow region at  $T_c$ .  $w$  also increases with  $T > T_c$ , and we find that once  $w \approx \pi$ , indicating significant entangling,  $n_c$  already gives at least one cutting per line. For  $T > T_c$ , we find  $w$  to have the same linear scaling with  $L_z$  as  $\langle u^2 \rangle$ ; hence we expect the ratio  $n_c/w$  of cutting to entangling to approach a constant as  $L_z \rightarrow \infty$ . In our model, vortex-line cutting can happen either in parallel (in which case two lines enter the same face of a unit cell, and that face has a vorticity of  $4\pi$ ) or perpendicularly (in which case the two lines enter perpendicular faces of the cubic unit cell, and each face has a vorticity of  $2\pi$ ). For  $1.5 > T > T_c \approx 1.0$  we observed only perpendicular cutting.<sup>13</sup>

We have also studied the effects of anisotropy, using a  $10 \times 10 \times 11$  lattice. For  $\gamma \equiv J_{\parallel}/J_{\perp} = 0.01, 0.075$ , and  $0.5$  we find  $T_c = 0.22, 0.35$ , and  $0.72$ , as determined by the location of the specific-heat peak. For  $\gamma = 0.01$ ,  $T_c$  lies close to that of the two-dimensional problem ( $\gamma = 0$ ), which has  $T_c \approx 0.18$ . Hence we have explored the complete range from nearly 2D behavior up to isotropic. Our results for  $n_c$  and  $w$  are plotted as functions of the rescaled temperature  $T/T_c(\gamma)$  in Fig. 4.  $n_c$  shows a comparable rise above  $T_c$  for all the anisotropies studied. The rise in  $w$  at  $T_c$  is steeper for the smaller  $\gamma$ , and can be attributed to crossover from the apparent second- (or weak first-) order transition of the isotropic 3D model to the first-order transition<sup>14</sup> of the 2D model. In all cases we find substantial vortex-line cutting when the lines are entangled.

Our lattice model (1) should be a good approximation for the continuum when the lattice constant  $a$  is small compared to other length scales, in particular the average spacing between vortex lines  $a_c$ . Our calculations have been carried out, however, at  $a_c = \sqrt{5}a$ , due to the need to have a sizable number of lines in a system small enough to simulate. At this high line density, the lattice plays a non-negligible role which makes quantitative comparison between our results and continuum melting theories<sup>1</sup> difficult. For example,  $\langle u^2 \rangle$  does not have the linear growth with  $T$  predicted by these models below

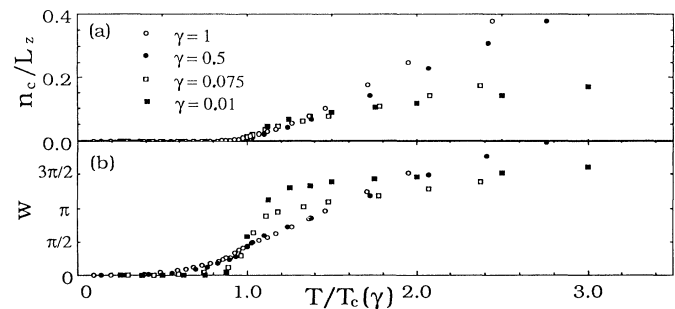


FIG. 4. (a) Cutting number per unit length  $n_c/L_z$  and (b) mutual pair winding number  $w$  vs  $T/T_c(\gamma)$  for different anisotropies  $\gamma \equiv J_{\parallel}/J_{\perp} = 0.01, 0.075, 0.5$ , and  $1$ . In each case, substantial vortex-line cutting is observed once the lines become entangled.

$T_c$ . We believe this is due to the effective periodic pinning potential which the lattice creates for the vortex lines. While we cannot therefore compare our value of  $T_c$  with the predictions of continuum Lindeman theories, our results for different anisotropies do fairly well fit the predicted scaling form,  $T_c/J_\perp \sim (J_\parallel/J_\perp)^{1/2} = \lambda_\perp/\lambda_\parallel$ . It is similarly difficult for our model to predict the nature of the phase transition at  $T_c$ , as this is likely affected by the commensurability of the ground-state vortex structure with the cubic lattice, such as occurs in 2D.<sup>8,9,14</sup> Nevertheless, it seems clear that fluctuations along the length of the vortex lines are important. In 2D (or  $\gamma \rightarrow 0$ ) we find hysteresis, indicating the transition is clearly first order;<sup>14</sup> however, for isotropic 3D we find no hysteresis, suggesting that the transition is either second or weakly first order. A second artifact of the lattice is that all transverse motion of the lines occurs by steps which are locally at right angles. At the relatively high density of lines considered here, this may enhance vortex-line encounters at large angles where the energy barrier for cutting is greatly reduced.<sup>15</sup> We have carried out similar calculations for the more dilute  $f = \frac{1}{7}$  model. In this case, the analysis is slightly more complicated as the ground-state vortex-line lattice is rectangular,<sup>8</sup> and thus has a lower symmetry. Nevertheless, we find the same qualitative behavior for  $\langle u^2 \rangle$ ,  $n_c$ , and  $w$  near  $T_c$  as for  $f = \frac{1}{5}$ . Numerical work on more dilute systems should help to clarify the relation between our lattice model and continuum superconductors. We point out, however, that for large line densities in layered high- $T_c$  materials, where  $\xi_0$  is often comparable to the spacing between layers, it is not obvious that the continuum is a better approximation than a lattice.<sup>16</sup>

We wish to thank Dr. M. Rubinstein, Professor Y. Shapir, and Professor D. R. Nelson for helpful criticism and discussion. This work has been supported by the U.S. Department of Energy under Grant No. DE-FG02-89ER14017. Computations were carried out as part of DOE sponsored research at the Florida State University Supercomputer Center.

<sup>1</sup>(a) D. R. Nelson and H. S. Seung, Phys. Rev. B **39**, 9153

(1989); (b) A. Houghton, R. A. Pelcovits, and A. Sudbø, Phys. Rev. B **40**, 6763 (1989); (c) E. H. Brandt, Phys. Rev. Lett. **63**, 1106 (1989); (d) M. A. Moore, Phys. Rev. B **39**, 136 (1989).

<sup>2</sup>D. R. Nelson, Phys. Rev. Lett. **60**, 1973 (1988); J. Stat. Phys. **57**, 511 (1989); D. R. Nelson and P. Le Doussal, Phys. Rev. B **42**, 10113 (1990).

<sup>3</sup>M. C. Marchetti and D. R. Nelson, Phys. Rev. B **42**, 9938 (1990); Physica C (to be published); S. P. Obukhov and M. Rubinstein, Phys. Rev. Lett. **65**, 1279 (1990).

<sup>4</sup>E. H. Brandt, in *Proceedings of the International Conference on Low Temperature Physics, LT-19*, edited by D. S. Betts [Physica (Amsterdam) **165 & 166B**, 1129 (1990)]; Int. J. Mod. Phys. B (to be published).

<sup>5</sup>M. V. Feigel'man, Physica (Amsterdam) **168A**, 319 (1990).

<sup>6</sup>E. Fradkin, B. Huberman, and S. Shenker, Phys. Rev. B **18**, 4789 (1978).

<sup>7</sup>More correctly, the lattice Green's function is  $V_q = 1/[6 - 2\cos(q_x) - 2\cos(q_y) - 2\cos(q_z)]$ , and similarly for the London interaction on a lattice.

<sup>8</sup>S. Teitel and C. Jayaprakash, Phys. Rev. Lett. **51**, 1999 (1983).

<sup>9</sup>S. Teitel and C. Jayaprakash, Phys. Rev. B **27**, 598 (1983).  
<sup>10</sup> $T_c^{MF} = T_c^{MF2D} + J_\parallel$ , where  $T_c^{MF2D} \approx 1.5$  is the mean-field transition temperature of the 2D model with  $f = \frac{1}{5}$ . See W. Y. Shi and D. Stroud, Phys. Rev. B **28**, 6575 (1983).

<sup>11</sup>Results for  $L_z = 5$  were obtained from simulations on a  $10 \times 10 \times 16$  lattice, where we have restricted the sum on  $z$  in Eq. (5) to a length  $L_z = 5$ , shorter than the length of the lattice.

<sup>12</sup>With periodic boundary conditions in the  $x$ - $y$  plane, the definition (7) of  $w$  is slightly ambiguous, since the  $\Delta \mathbf{r}$  are undefined modulo  $L$ . To make (7) precise, we choose the following convention. For any given pair of vortex lines we measure their positions  $\mathbf{r}_i(z)$  such that the  $|\min_z \Delta \mathbf{r}(z)| \leq L/2$ . All other  $\Delta \mathbf{r}(z)$  for this pair are measured relative to this choice. Near  $T_c$ , where  $\langle u^2 \rangle^{1/2} \ll L$ ,  $w$  should be insensitive to this particular convention.

<sup>13</sup>We can estimate the energy barrier  $\Delta E$  for parallel cutting as follows. Using the 2D lattice Green's function with periodic boundary conditions, given by  $\nabla_i^2 G(\mathbf{r}_j - \mathbf{r}_k) = \delta_{jk}$ , to give the interaction energy between parallel lines, we find  $\Delta E \approx -2\pi^2 \times [G(\sqrt{5}) - G(0)] \approx 7.4 \gg T_c$ . For  $1.5 < T < 2.5$  we found the number of parallel cuttings to be  $< 0.3\%$ .

<sup>14</sup>Y. H. Li and S. Teitel (to be published).

<sup>15</sup>E. H. Brandt, J. R. Clem, and D. G. Walmsley, J. Low Temp. Phys. **37**, 43 (1979).

<sup>16</sup>J. R. Clem, Phys. Rev. B **43**, 7837 (1991).